Fabrication and properties of Rapidly Solidified Powder-based high-temperature application light-alloy composites

N. RAGHUNATHAN, H. B. McSHANE, C. DAVIES, T. SHEPPARD
Department of Materials, Imperial College of Science, Technology and Medicine, London SW7 2AZ, UK

Particulate-reinforced composites based on Al–Fe–Ce and SiC were fabricated by conventional powder metallurgy techniques, namely powder mixing, cold compaction and hot extrusion. Static mechanical properties at ambient temperature and at elevated temperature after prolonged exposure to the test temperature were measured and related to process parameters and the volume fraction of the reinforcement. The addition of SiC particles in considerable volume fractions help to retain the static properties at high temperature, even after prolonged exposure. It was also observed that the mechanical strength increases with decreasing temperature and extrusion ratio. Unavoidable non-uniform distribution of SiC particles and the associated porosity were observed to be responsible for wide variations in the properties within the same extrudate. Attempts to reduce this variation are discussed.

1. Introduction

Conventional high-strength aluminium alloys, such as the 2XXX and 7XXX series alloys, lose their strength at an increasing rate above 150° C due to coarsening of the strengthening precipitate with the attendant loss of coherency with the matrix. However, by introducing stable dispersoid formers by the use of transition metals or rare earth elements, the loss of strength at elevated temperatures can be reduced, resulting in improved mechanical properties up to 350° C. The mechanisms of strengthening at elevated temperature in such cases are different and depend upon the stability of dispersoids and resistance to coarsening at high operating temperatures. The stability is determined by the diffusivity and the solubility of the dispersoid-forming element in the aluminium matrix. In this respect the transition and rare earth elements offer the opportunity of designing aluminium-alloys for elevated temperature service.

Two alloy systems based on Al–Fe–X or Al–Cr–X, where X can be one or more of molybdenum, vanadium, cerium, silicon, nickel or zirconium, are currently under investigation in several laboratories. These alloys are produced either in powder form by gas atomization or by substrate quenching in ribbon form followed by comminution by pulvarizer. The materials produced by either method are considerably stronger than conventional aluminium alloys; a direct result of the presence of transition phases and refined microstructure developed during production. Hence these materials require significantly higher temperatures or forces for final consolidation by extrusion or forging. The consequence of applying high temperatures [1] for processing is the weakening of the consolidated component due to the precipitation of dispersoid formers

in a form unsuitable for strengthening and coarsening of existing dispersoids in the powder. Attempts to consolidate these materials at low temperatures have met with failure due to the limited press force available or due to poor quality of the product. This essentially restricts the processing "window" to high-temperature regions when existing presses are utilized. Recently, some attempts have been made to improve the high-temperature strength by alternative means [2]. One such method is by consolidation at high temperature but with additions of inorganic compounds such as carbides, oxides, borides or even stable intermetallic compounds, to compensate for the loss of strength due to the high processing temperature.

In this paper we report the results of experiments carried out at Imperial College to improve the mechanical properties of a high-temperature Al–Fe–Ce generic alloy by incorporating various volume fractions of SiC particles. The composites were fabricated by conventional powder metallurgy (P/M) methods. The aim was to produce a material which could retain a proof stress of 300 MPa after prolonged exposure at 315° C by suitable combinations of processing parameters and compositions.

2. Materials processing

The alloy powder was supplied by Alcoa, USA, and had the composition Al–8.27 Fe–3.81 Ce–0.11 Si–0.8 Mn–0.02 Cu (wt %). The powder was predominantly spherical, typical of a gas-atomized powder, and was sieved at 75 μm, giving a median particle size of 25 μm.

The reinforcement SiC powder was supplied by Sohio Ltd, UK. The powder was 99% pure with the remaining 1% being SiO_2 and Al_2O_3. The powder particles had acicular morphology with sharp corners,
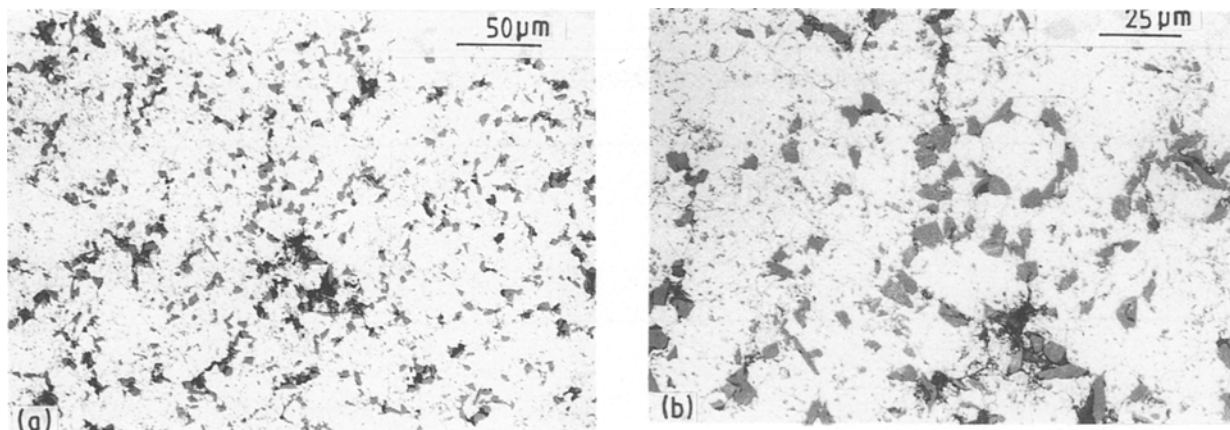
Figure 1 SiC particle distribution in the cold compact. The volume fraction of SiC is 10%.

typical of milled powder, and had a median particle size of 5 μm with the particle size spectrum ranging from 2 to 13 μm.

Mixing of the powders was carried out in house at Imperial College in a proprietary mixer. The silicon carbide powder was dried to facilitate mixing. A series of experiments was conducted to obtain the best mixing conditions.

The powder mixtures were consolidated in two stages. In the first stage, the powders were poured into a die steel container (75 mm diameter), coated with zinc stearate and compacted cold into small billets of 75 mm diameter and 80 mm length with an applied pressure of 400 MPa in a 1.5 MN uniaxial press. The cold-compacted billets were subsequently pre-heated in an air-circulating furnace prior to extrusion to the required temperature and extruded into round bars of 12 mm diameter in a 5 MN vertical extrusion press, giving an extrusion ratio of 40:1 in the process. A range of temperatures from 350 to 500° C was used to investigate the influence of process temperature upon the mechanical properties. In an effort to extrude at lower temperatures, the initial billet diameter and the container size of the extrusion press were changed from 75 to 52 mm, which increased the available pressure from 1100 to 1500 MPa. This necessarily changed the extrusion ratio from 40:1 to 18:1 for the same product size. Two different volume fractions, 10 and 20 vol %, of SiC were studied in the present set of experiments. Additionally some metal powder compacts without reinforcement were processed under identical conditions to evaluate the base-level properties.

3. Material evaluation

Both the mechanical properties and the microstructure were evaluated at various stages of processing to assess the influence of processing parameters. Static mechanical strength properties were evaluated at room temperature and at elevated temperature using non-standard round tensile bar specimens, machined from the extrudates. The samples for the high-temperature testing were heat treated prior to testing for an extended period of 100 h. Some selected samples were given a further heat treatment of 400 h at the test temperature. The microstructures of the extruded materials were investigated using optical and

scanning electron microscopy. Examination of the fracture surfaces of the tensile samples was carried out in a Jeol T220A scanning machine.

4. Results and discussion
4.1. Fabrication

Mixing of the powders prior to consolidation is the most critical in determining the homogeneity of the reinforcement distribution in the final product. This depends upon various factors including the flow of individual powders, the relative density, the relative particle size distribution, the type of mixer and the time of mixing. In the present case for the given powders, it has been observed that dehydration of the SiC powders enhances the mixing ability, mainly because it increases the flowability. The aluminium powders could not be heat treated because this might induce undesirable structural features. The distribution of SiC particles in the cold compact are shown in Fig. 1. It can be seen that the SiC particles are distributed almost uniformly along the metal/particle boundaries. In some areas the SiC particles have agglomerated, especially at the triple-point particle/boundary junctions, resulting in porosity (Fig. 1b). Increasing the pressure of compaction eliminates some of these pores by extrusion of the metal powder particle into the crevices. Subsequent hot extrusion results in an almost pore-free product.

The maximum green density obtained in the composites after cold compaction varied between 65% and 70% theoretical density at the highest pressure (400 MPa). This is in contrast to 90% to 92% green density of the unreinforced metal powder compacts. The consequence of this difference in the porosity level in the composite compacts is that the compact could not be preheated in an induction heater. The billets were hence preheated in an air-circulating furnace for 40 min to obtain a uniform temperature.

The extrusion of the composite billets through a flat-faced die posed considerable difficulties due to surface cracking at all temperatures and speeds. Some form of lubrication was therefore necessary. By using graphite dispersed in an oil medium, it was possible to extrude the billets at low speeds. The extrudates contained no cracks, though coarse die lines were observed on the surfaces of all specimens.

TABLE I Mechanical properties of base material Al–Fe–Ce

Extrusion temperature (°C)	Test temperature (°C)	Extrusion ratio	Proof stress	UTS (MPa)	% elongation
440	20	20	380 ± 9	438 ± 5	6 ± 2
490	20	20	353 ± 5	422 ± 2	10 ± 1
540	20	20	298 ± 2	367 ± 2	15 ± 5
440	315	20	224 ± 9	249 ± 15	12 ± 4
490	315	20	216 ± 5	239 ± 9	18 ± 2
540	315	20	185 ± 5	208 ± 3	20 ± 4

4.2. Mechanical properties and microstructure

The basic mechanical properties of the as-extruded as well as heat-treated samples of composite and unreinforced materials are given in Tables I and II. The presence of superficial or subcutaneous defects such as pores restricted the data collection due to premature failure of specimens.

The data shown in Tables I and II are taken from samples that deformed fully into the plastic state. In comparing the improvements in the properties of the composite over the base material, as shown in Tables I and II, it should be pointed out that some of the processing parameters are not equivalent, i.e. the unreinforced materials in Table I experienced an extrusion ratio of 20:1, while the composites were extruded at 17:1 and 40:1 ratios.

Typical load–elongation curves observed in the present set of tensile tests at room temperature are shown in Fig. 2. All curves show a small initially linear elastic region followed by a fully developed non-linear elastic–plastic region. It is generally accepted that metal matrix composites fabricated at high temperatures exhibit distorted linear elastic portions in their

tensile curves or in some cases this portion is completely absent which is presumably due to the residual stresses introduced during quenching from high temperatures as a result of differential thermal expansion of the reinforcement and the matrix. Measurements of the Young's modulus in the linear region on some selected samples indicated that the values increase from 106 ± 18 to 118 ± 13 GPa for 10 vol % reinforcement, to 140 ± 24 GPa for 20 vol % reinforcement at room temperature for the material extruded at 540° C with an extrusion ratio of 40:1.

Reference to Tables I and II indicated that the room-temperature proof stress measured at 0.2% permanent strain and the ultimate tensile stress increased substantially on incorporation of various volume fractions of SiC. The properties, however, increased disproportionally with increasing volume fraction of SiC. It is also observed that the strength parameters change with extrusion temperature. The above increase is also accompanied by a substantial reduction in the percentage elongation. While the strengthening of the base matrix due to the reinforcement by SiC particles remains undisputed, the exact nature of the mechanisms of strengthening by medium-sized particles, as in

TABLE II Mechanical properties of Al–Fe–Ce + SiC composite

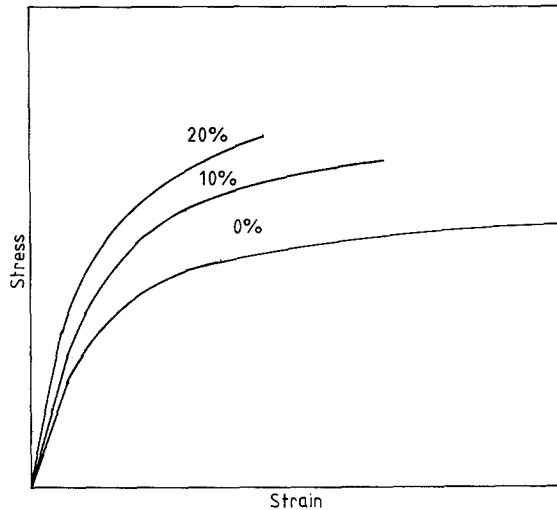| Extrusion temperature (°C)	Extrusion ratio	Test temperature (°C)	Proof stress (MPa)	UTS (MPa)	% elongation	Volume fraction
440	17:1	20	447 ± 5	492 ± 4	2 ± 2	10
440	17:1	20	463 ± 11	512 ± 7	<1	20
500	17:1	20	363 ± 10	413 ± 11	6 ± 1	10
500	17:1	20	413 ± 12	469 ± 2	<1	20
540	40:1	20	220 ± 5	313 ± 8	14 ± 3	0
540	40:1	20	270 ± 10	362 ± 4	4 ± 1.5	10
540	40:1	20	300 ± 10	435 ± 4	3 ± 2	20
440	17:1	200	320 ± 1	345 ± 3	6 ± 2.5	10
440	17:1	200	372 ± 13	393 ± 6	6 ± 1.5	20
500	17:1	200	304 ± 3	318 ± 6	7 ± 3	10
500	17:1	200	371 ± 4	387 ± 4	5 ± 1.3	20
540	40:1	200	195 ± 2	220 ± 3	15 ± 3	0
540	40:1	200	231 ± 5	250 ± 2	12 ± 2	10
540	40:1	200	273 ± 5	300 ± 4	7 ± 4	20
440	17:1	315	208 ± 3.5	220 ± 3.5	11 ± 3.5	10
440	17:1	315	225 ± 12	230 ± 13	9 ± 1	20
500	17:1	315	185 ± 7	195 ± 8	9 ± 1.5	10
500	17:1	315	213 ± 1	232 ± 1	9 ± 3.5	20
540	40:1	315	142 ± 0	155 ± 4	13 ± 0	0
540	40:1	315	181 ± 10	192 ± 9	9 ± 2.5	10
530	40:1	315	206 ± 7	216 ± 14	7 ± 0	20
540*	40:1	315	145 ± 4.5	152 ± 5	18 ± 4	0
540*	40:1	315	168 ± 11	178 ± 4	10 ± 2	10
540*	40:1	315	195 ± 4	212 ± 4	6 ± 3	20

*Samples heat treated for 500 h.

*Figure 2* Schematic illustration of the type of stress–strain curves obtained in the present research.

Figure 3 Transmission electron micrograph of a 440° C extrudate showing two undeformed powder particles. The direction of extrusion is parallel to the plane of the micrograph.

the present case, is still not clear. The size spectrum of the SiC particles used implies that matrix strengthening is not caused by the classical Orowan mechanism. At the same time the particle size is not coarse enough for a load-sharing or strain-partitioning mechanism [2] to operate.

Two important observations of the above data are that all properties, especially the elongation, show considerable variation from sample to sample and that the modulus of the unreinforced material is much higher than any conventional aluminium alloy. To understand these variations it is necessary to look into the microstructure of the extrudate and any inhomogeneity in the structure will obviously affect the properties. Two major types of inhomogeneity must be considered. The first is microstructural inhomogeneity inherited in the product from the parent metal powder. The second tyupe of inhomogeneity in the extrudate is the presence of undeformed fine metal particles. Powders produced by atomization undergo different thermal and solidification histories depending on the size of the individual particles. As a result, the solidified structures vary from particle to particle. The structural variations are summarized below [1].

(a) Powders under $8 \mu m$ mean particle size contained almost exclusively microcellular structures with an α solid solution of iron or cerium in aluminium forming the microcells surrounded almost continuously by $Al_x Fe_y Ce_z$ metastable ternary intermetallic phase in the intercellular regions. There was no evidence of segregation-free, partitionless solidification similar to that observed in a pure Al–Fe binary [3].

(b) In medium-sized particles (-25 to $+12 \mu m$) microcellular structures were found close to the nucleation centre. These gradually changed to a coarse cellular morphology away from the nucleation centre with the intercellular ternary phase $Al_x Fe_y Ce_z$ changing in composition from inter-microcellular regions to inter-cellular regions.

(c) In powder coarser than $30 \mu m$, precipitated primary $Al_x Fe_y$ binary phase dispersoids of size $> 0.5 \mu m$ act as nucleants for solidification of coarse cells of
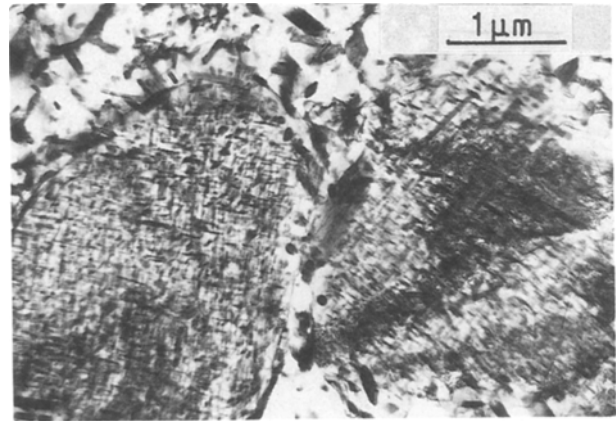
α-Al solid solution with the ternary $Al_x Fe_y Ce_z$ phase in the intercellular regions.

The application of pressure and temperature, during extrusion, to the powder compacts containing a wide spectrum of particle sizes results in certain changes to the microstructure of the powder particles. Firstly, during extrusion of powder compacts containing fine and coarse powder particles, coarse particles deform preferentially with respect to fine particles. The fine particles in such instances assume a similar role to that of a hard second phase. In an extreme case undeformed powder particles can be observed in the product (Fig. 3). However, on increasing the process temperature or extrusion ratio, such heterogeneities occur less frequently. The presence of such heterogeneities will impair the fracture properties considerably. The second type of heterogeneity observed is shown in Figs 4a, b and 5a, b for materials extruded at low temperatures and high temperatures. The microcells in the fine powders, supersaturated with transition metals precipitate the excess solute in a typical widmanstatten pattern, Fig. 4b, exhibiting a habit-plane relationship of (1 0 0) with aluminium. An increase in the extrusion temperature or extrusion ratio results in a coarser distribution of the above observed platelets and at considerably higher temperatures the precipitates lose their crystallographic relationship with the matrix aluminium. The coarse cells which are much less supersaturated with respect to the fine cells, show no response in terms of precipitation of the transition elements. The ternary intercellular intermetallic phase undergoes phase transition to a more stable form ($Al_{10} FeCe_2$ or $Al_8 Fe_4 Ce$), while the primary $Al_x Fe_y$ metastable binary in coarse particles undergoes transition to a stable $Al_3 Fe$ or metastable $Al_6 Fe$ structure. The outcome of the hot extrusion of the compact containing a wide range of particle sites is that the extrudate contains some fine undeformed particles with the widmanstatten microstructure, embedded in a continuum of elongated coarse particles of α-solid solution. Additionally the extrudates will contain profuse quantities of binary Al–Fe and ternary Al–Fe–Ce particles inhomogeneously distributed. These particles are inherently stiffer due to their complex crystal structure.
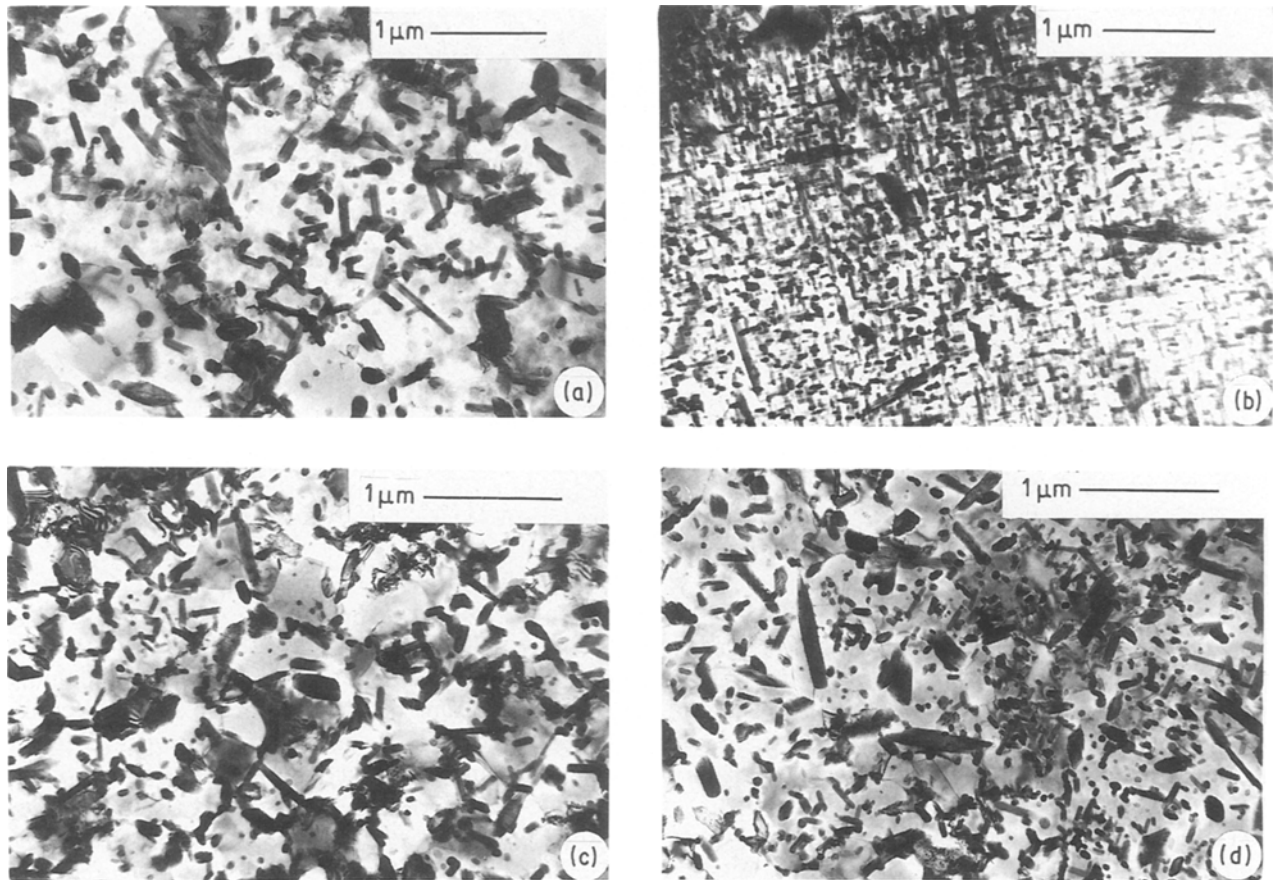
4909

Figure 4 Transmission electron micrographs of a 440° C extrudate showing typical microstructural inhomogeneities in the as-extruded condition (a), (b), and after 100 h exposure to 315° C (c), (d).
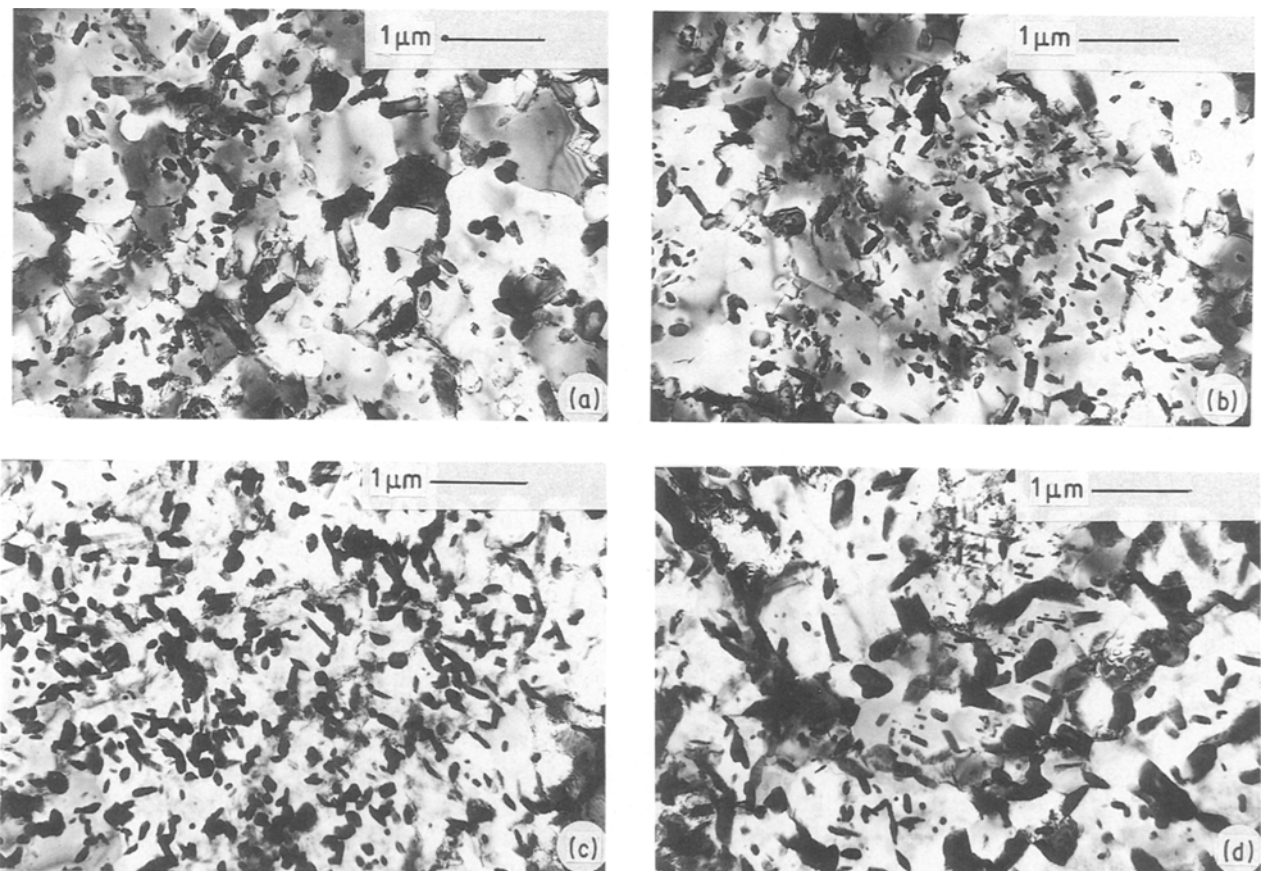

Figure 5 Transmission electron micrographs of a 550° C extrudate showing structural inhomogeneities in the as-extruded condition (a), (b), and after 100 h exposure to 315° C (c), (d).
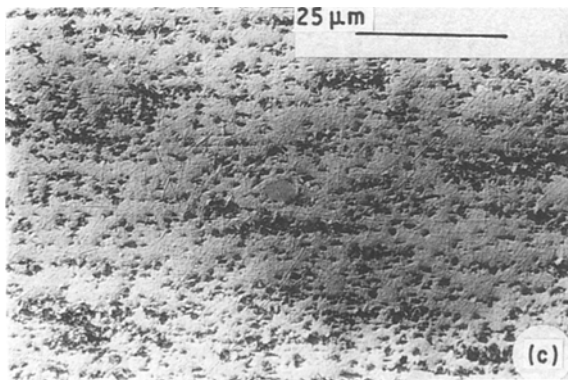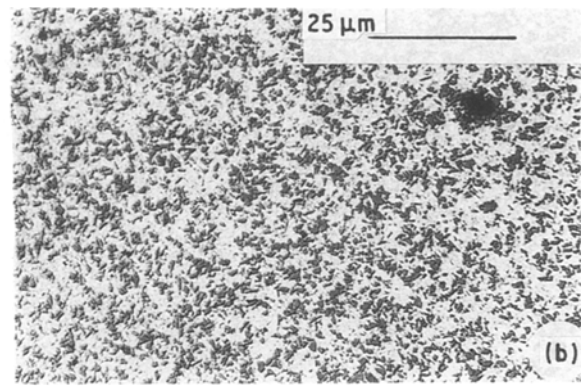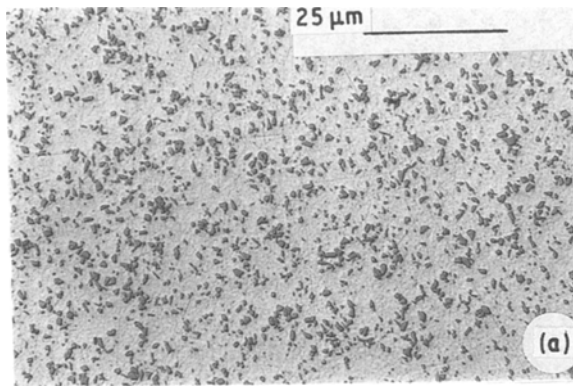
Figure 6 SiC particle distribution in a 500° C extrudate. Transverse section of the extrudate with (a) 10 vol % and (b) 20 vol % SiC. Note the porosity associated with the particles in (b). (O) Longitudinal section of the extrudate with 20 vol % SiC.

The higher modulus (106 ± 18 GPa) of the base material reported above as compared to commercial purity aluminium can be related to the volume fraction of these individual dispersoids. Also the variations in the properties both in strength and modulus can be explained on the basis of the inhomogeneities discussed above.

In composite materials, another source of microstructural heterogeneity arises from the distribution of SiC particles. Fig. 6 shows the distribution of SiC in the extruded material as a function of volume fraction of SiC. It can be seen that the SiC particles aligned uniformly around the original particle boundary in the cold compact are strung out in the direction of extrusion (Fig. 6c). In some cases SiC particles are so close, especially at higher volume fractions of SiC, that some residual porosity remains (Fig. 6b). Such material, when subjected to loading parallel to the extrusion direction, will have varying properties as the effective load-carrying area is reduced by the porosity. If the loading is transverse to the extrusion direction such pores will act as stress concentration sources. It is interesting to note that such pores are observed only in the centre of the extrudates. Increasing the extrusion temperature or extrusion ratio helps to annihilate this porosity by allowing the matrix material to flow through the crevices of an agglomerated region and disperse the particles. Thus high temperature and extrusion ratio are desirable from this point of view. Tables I and II indicate, however, that an increase in these parameters weakens the matrix. An increase in the extrusion ratio results in greater heat generated during extrusion due to the conversion of deformation energy to thermal energy. Thus an optimum combination of processing conditions must be selected.

The main interest of the present investigation is in the behaviour at high temperature of the composites. The proof stress and the ultimate tensile stress are plotted in Figs 7a to c as functions of test temperature. Both properties follow the same trend, i.e. they decrease with increasing test temperature. The rate of decrease of the strength with increasing test temperature depends upon various factors such as extrusion temperature, extrusion ratio and volume fraction of reinforcement. In plotting the data it was presumed that the variations in extrusion ratio had negligible effect on the properties at high temperature. One of the reasons for the prolonged heat treatment given in these experiments is to facilitate a considerable amount of coarsening with the resultant loss of strength so that the properties of these specimens would have the minimum attainable value and could be used as a reference point. The intent of adding SiC particles is to reduce this loss of strength at high temperature as a result of coarsening of constituent particles.

The resulting microstructures after prolonged heat treatment are shown in Figs 4c, d and 5c, d. One obvious conclusion is that coarsening occurs in all extrudates to varying degrees. Thus the material extruded at high temperature had a lower coarsening rate, presumably because the parent microstructure before heat treatment itself is much coarser. There are two parameters involved in the coarsening and the associated loss of strength. One is that average constituent particle size and interparticle distance increases and the other is that the matrix of α-solid solution undergoes large-scale static recovery. Both contribute to the loss of load-bearing capacity and both depend on the time and temperature of heat treatment. However, increasing the time from 100 to 500 h had only a slightly deleterious effect (Table I), in the present case. This effect has been tested only for the material extruded at 540° C which has an inherently lower coarsening rate due to the coarse scale of the as-extruded microstructure. Another trait common to both base material and the composites is that the ductility increases considerably at high temperature. Thus the loss of ductility due to the additions of SiC or extruding at low temperature assumes less
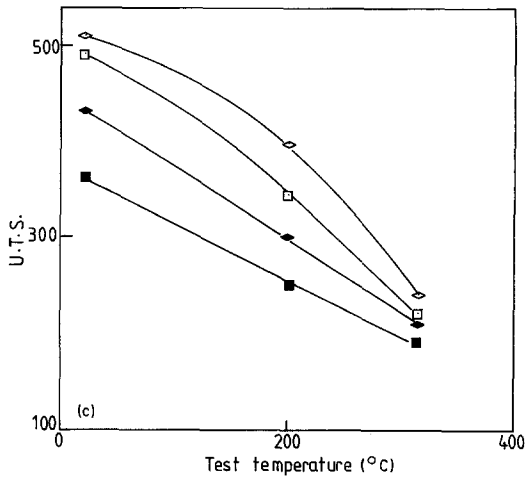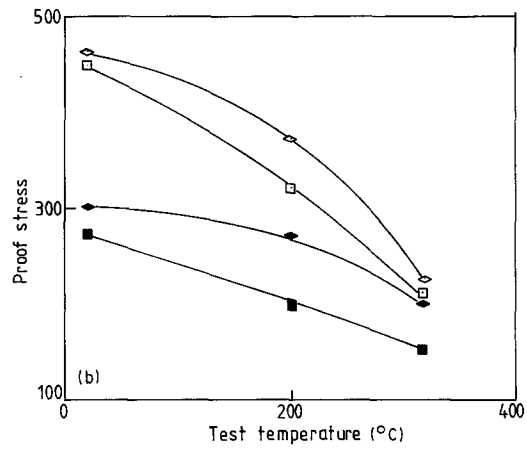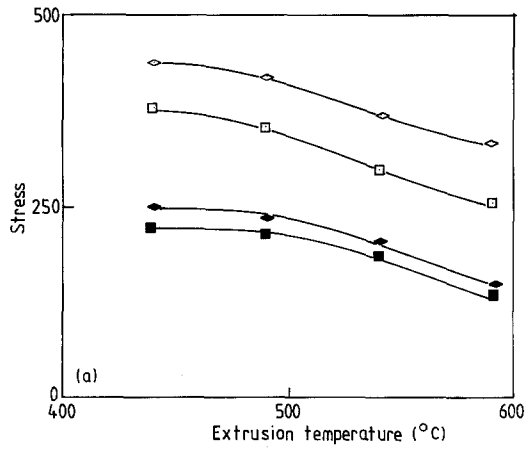
Figure 7 Static mechanical properties of the extrudate: (a) matrix properties (□, ■) Proof stress and (◇, ◆) UTS at (□, ◇) 20°C, (■, ◆) 315°C; (b), (c) composite properties, extrusion temperature: (□, ◇) 440°C, (■, ◆) 540°C for (□, ■) 10 and (◇, ◆) 20 vol% SiC.

importance when the material has an elevated temperature application.

The fracture surfaces of both unreinforced and reinforced samples are shown in Figs 8 and 9, respectively, for the room-temperature and high-temperature test specimens. The main features observed in the base material and the composite materials are large amounts of secondary cracking and delamination along the original particle boundaries aligned in the direction of extrusion. Elsewhere the matrix material showed dimpled fracture indicative of matrix ductility. In the composites the fracture initiation point was almost always an agglomeration of SiC particles or the pore associated with it. It is worth noting that SiC particle agglomeration has two sources. One is due to poor mixing and distribution, while the other is present already in the parent SiC powder known as "hard agglomerates". The first type of agglomeration is removable by improving mixing conditions and the other depends upon the quality of commercially available parent powder. In summary, an improvement in
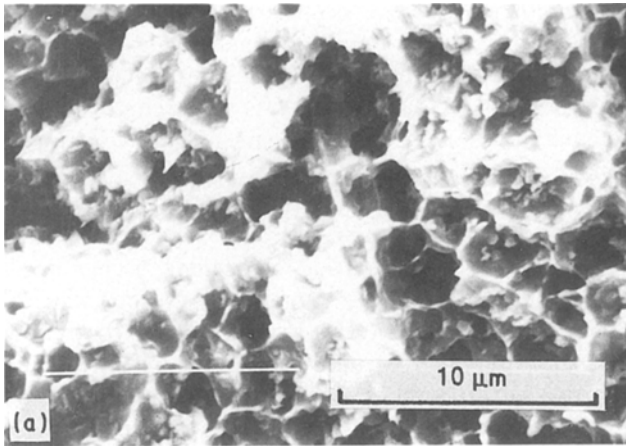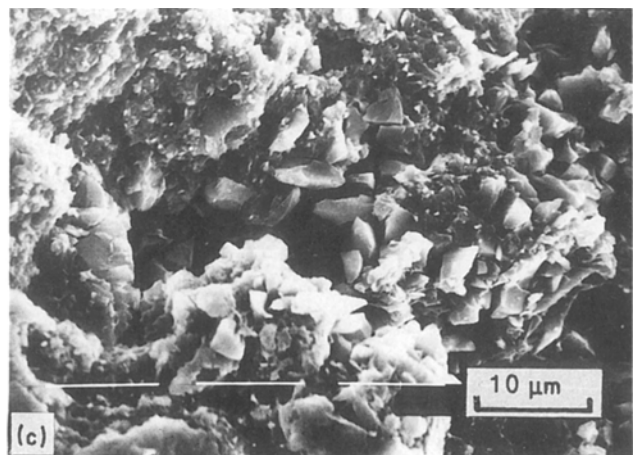

Figure 8 Fractographs of room temperature tensile specimens: (a) matrix; (b), (c) composite with 20 vol% SiC. Notice the fracture associated with the agglomeration of SiC along the boundary of the metal/powder particle.
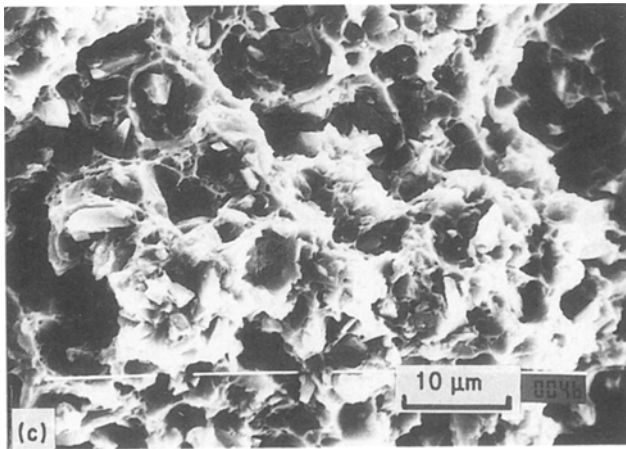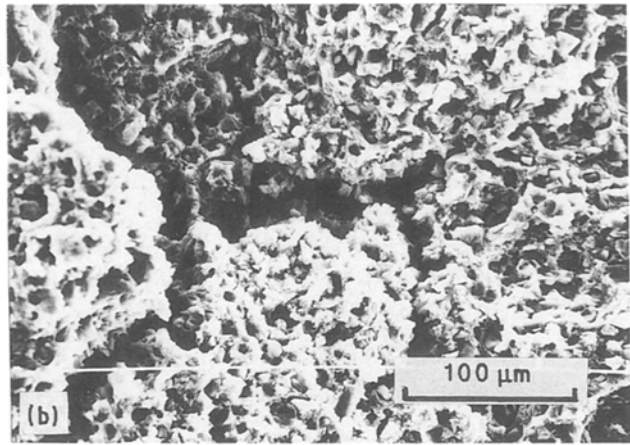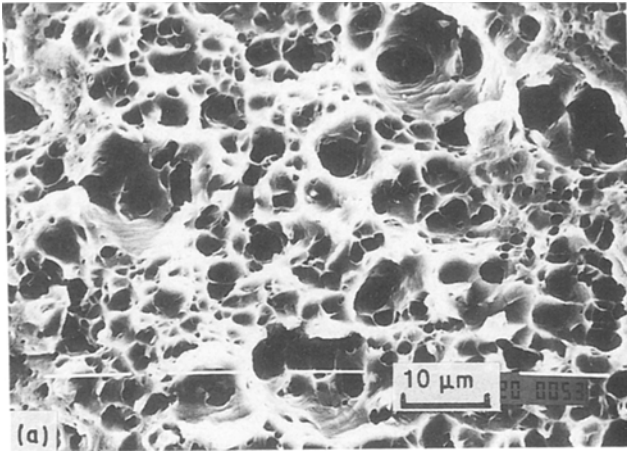
Figure 9 Fractographs of 315° C tensile specimens: (a) Matrix showing extensive ductility; (b) Composite containing discontinuous cracks along the extruded particle boundary. The extrusion direction is normal to the plane of the micrograph. (c) The dimple associated with the SiC particles along one of the metal/powder particle boundaries.

the absolute mechanical properties and a decrease in the net loss of strength at high temperatures have been obtained by increasing the volume fraction of SiC reinforcement and utilizing both low extrusion temperatures and low extrusion ratios.

5. Conclusions

The objective of this work was to investigate how much the high-temperature strength of Al–Fe–Ce P/M alloy can be improved by the incorporation of SiC particulates and to obtain a material having a proof stress of 300 MPa at 315° C after prolonged exposure to temperature. With regard to the second objective, the data are inconclusive. The present data indicate that beyond 250° C the loss of strength occurs at an accelerated rate in the composites compared to the base metal, even though the absolute levels of strength in the composites are higher. However, projection of the data indicates that increasing the SiC volume fraction from 20 to 30 vol % and extruding preferably around 450° C with an extrusion ratio of 15

to 20 may have the potential to yield the required property. It has also been shown that coarsening, which is responsible for loss of strength at high temperature in the base metal, does not pose a problem in the composite containing a considerable volume fraction of SiC. Also, ductility is not a problem as it is observed to increase at high temperature and the volume fraction of SiC has a much smaller effect on the ductility at high temperature. It should be noted that the above property improvements occur at the cost of increasing the density. The variation in the properties from sample to sample in the composites is wider than in monolithic aluminium alloys and this, of course, is detrimental to the quality control. This variation is related to the defect density, nature of defect, and type of loading. In the present case, defects such as agglomerates of SiC particles and the pores associated with them or undeformed fine metal powder particles are found to be present in the material. Their numbers can be reduced by increasing the process temperature considerably or by increasing the extrusion ratio.

References
1. T. SHEPPARD and M. A. ZAIDI, *Mater. Sci. Techn.* **2** (1986) 69.
2. J. W. MARTIN, "Micromechanisms in Particle Hardened Alloys" (Cambridge University Press, 1980) pp. 50–98.
3. W. J. BOETTINGER, *Met. Trans.* **17A** (1980) 781.